Synthesis and electron-transfer properties of benzimidazole-functionalized ruthenium complexes for highly efficient dye-sensitized solar cells†

Wei-Kai Huang,[a] Chi-Wen Cheng,[a] Shu-Mei Chang,[b] Yuan-Pern Lee[a] and Eric Wei-Guang Diau*[ac]

Novel heteroleptic ruthenium complexes—RD1, RD5, RD10 and RD11—with ligands based on benzimidazole were synthesized and characterized for application to dye-sensitized solar cells (DSSC); the remarkable performance of RD5-based DSSC is understood for its superior light-harvesting ability and slower charge-recombination kinetics.

Dye-sensitized solar cells (DSSC) have attracted attention because of their efficient performance, ease of fabrication and economy of production.[1] Much effort has been devoted to the synthesis and characterization of various sensitizers for DSSC, such as ruthenium complexes,[2] zinc porphyrins[3] and metal-free organic dyes.[4] The devices made of ruthenium polypyridyl complexes, such as N3 and N719 dyes, attained an efficiency ∼11% of power conversion under one-sun illumination.[5] To improve the efficiency of light harvesting, heteroleptic ligands based on thiophene were designed to make ruthenium complexes with large absorption coefficients, thus enhancing the efficiency of the device to 11.5%.[6] The synthesis of those thiophene-based ligands was, however, more elaborate than for the commercial N719 dye. Because their electron mobilities are great, benzimidazole derivatives have been developed as layer materials for electron transport and hole blocking in organic light-emitting diode devices.[7] Bearing a similar idea in mind, we designed heteroleptic ruthenium complexes containing benzimidazole substituents in a series for which the corresponding ligands can be synthesized in a simple two-step procedure.

Here we report four novel heteroleptic ruthenium complexes, RD1 [Ru(dcbpy)(1-methyl-2-(pyridine-2-yl)benzoimidazole)-(NCS)₂], RD5 [Ru(dcbpy)(1-benzyl-2-(pyridine-2-yl)benzo-imidazole)(NCS)₂], RD10 [Ru(dcbpy)(1-decyl-2-(pyridine-2-yl)-benzoimidazole)(NCS)₂] and RD11 [Ru(dcbpy)(1,1′-dimethyl-2,2′-bibenzoimidazole)(NCS)₂], for which one 4,4′-dicarboxylic-2,2′-bipyridine (dcbpy) ligand in N3 dye was replaced by a heterocylic ligand (Chart 1). The DSSC device made of RD5 sensitized on the TiO₂ film exhibits photovoltaic performance comparable with the specifications of a device made of N719

dye. The results obtained from photocurrent and photovoltage decays indicate that the electron lifetimes of the devices display a systematic trend RD5 > RD10 > RD1 > RD11, which is consistent with the cell performance in the same order. Femtosecond measurements of infrared transient absorption (TA) of the samples as thin films indicate that, for RD-series sensitizers there exists a decay component on a ns time scale representing the back-electron transfer (BET) occurring at the interface between TiO₂ and dye, whereas for dye N719 such a process was not observable. Combining results from both electron-transfer kinetics reasonably explains the order of V_{OC} to be N719 > RD5 > RD10 > RD1 > RD11. In contrast, the IPCE action spectra of the devices account for the order of J_{SC} to be RD5 > N719 > RD10 > RD1 > RD11. The superior performance of RD5-based DSSC is thus understood for its superior light-harvesting ability and charge-recombination kinetics.

Fig. 1 shows the absorption spectra of RD1, RD5, RD10, RD11 and N719 in DMF; the corresponding spectral (Fig. S1†) and electrochemical (Fig. S2†) properties of these dyes are listed in Table S1.† The UV-visible absorption spectra of these complexes exhibit a band to the red of the corresponding band for dye N719. Even though the molar absorption coefficients ($\varepsilon/M^{-1} cm^{-1}$) of RD1 (7560 at 539 nm), RD5 (8005 at 537 nm), RD10 (7796 at 537 nm) and RD11 (6483 at 538 nm) are significantly smaller than that of N719 (13610 at 524 nm), the absorbances of the corresponding thin-film spectra on TiO₂ films are slightly greater than that of N719 (inset of Fig. 1). This property reflects that the amounts of the RD series dyes adsorbed on TiO₂ surface are significantly greater than that of N719 (Table 1).

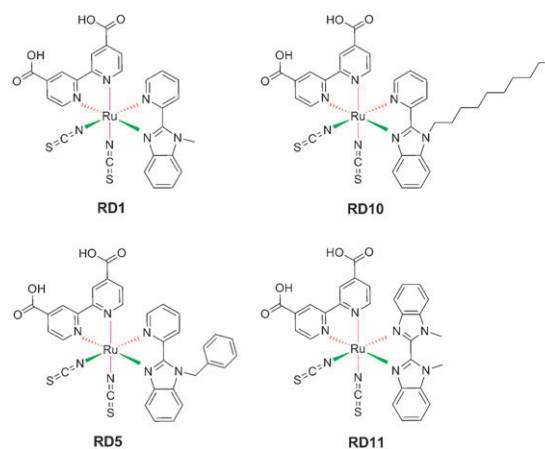[a] Department of Applied Chemistry and Institute of Molecular Science, National Chiao Tung University, Hsinchu 300, Taiwan. E-mail: diau@mail.nctu.edu.tw; Fax: +886 3-572-3764; Tel: +886 3-513-1524
[b] Institute of Organic and Polymeric Materials, National Taipei University of Technology, Taipei 106, Taiwan.
[c] On sabbatical leave in Department of Chemistry, University of Copenhagen, DK-2100 Copenhagen, Denmark
† Electronic supplementary information (ESI) available: Supplementary figures (Fig. S1–S3), tables (Tables S1–S2) and experimental details. See DOI: 10.1039/c0cc03517c
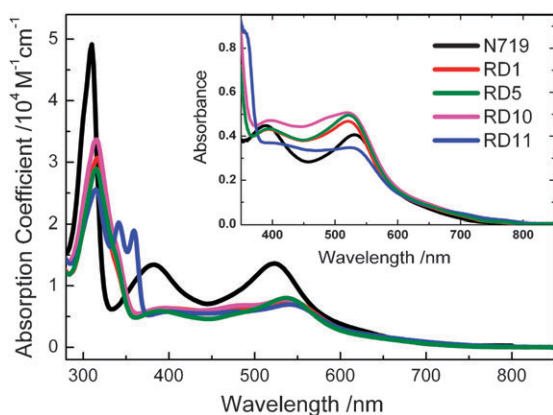

Chart 1 Molecular structures of RD1, RD5, RD10 and RD11.

Fig. 1 Absorption spectra of **RD1**, **RD5**, **RD10**, **RD11** and **N719** in DMF. Inset shows absorption spectra of TiO_2 films (active layer of thickness 2 μm) sensitized with the indicated dyes.

Fig. 2a compares the current–voltage characteristics of these four dyes on TiO_2 films of thickness 12 + 3 μm with that of **N719** under the same conditions of device fabrication; the corresponding photovoltaic parameters are listed in Table 1. The values of V_{OC}/V are 0.694 for **RD1**, 0.737 for **RD5**, 0.710 for **RD10** and 0.685 for **RD11**, showing the effect of various substituents on the imidazole ring and the effect of the bibenzimidazolyl ligand. The values of J_{SC}/mA cm^{-2} are 12.744 for **RD1**, 15.084 for **RD5**, 13.612 for **RD10** and 11.159 for **RD11**. This variation of J_{SC} is inexplicable solely as the effect of dye loading. The trend of J_{SC} is, however, consistent with the variation of IPCE shown in Fig. 2b. As mentioned for the absorption spectra, the IPCE action spectra of dyes in the **RD** series exhibit also a red-shifted spectral feature beyond 800 nm, in particular for **RD5** showing greater efficiency and breadth than those properties of **N719**. The total efficiency of power conversion of **RD5** attains 7.7%, which is comparable with that of **N719** ($\eta = 7.8\%$). The **RD5** device performed slightly better than the **N719** device with the thinner TiO_2 films (Fig. S2† and Table S2†) because of the superior dye-loading effect of **RD5**.

Fig. 3a and b show the electron-transport kinetics of the corresponding devices obtaining from an analysis of the photovoltage (Fig. 3a) and photocurrent (Fig. 3b) decay data.[8] The electron-diffusion coefficients (D) are similar for each dye, but the time coefficients for electron recombination (τ_R) display a systematic trend **RD5** > **RD10** > **RD1** > **RD11**. This trend indicates that charge recombination between the dye (or I_3^-) and the TiO_2 surface might occur near the imidazolyl ligands. The existence of a hydrophobic chain in the imidazolyl ligand (**RD10**) longer than for dye **RD1**,

Table 1 Photovoltaic parameters and amounts of dye loaded on DSSC with TiO_2 films sensitized with **RD1**, **RD5**, **RD10**, **RD11** and **N719** under simulated AM-1.5G illumination (100 mW cm^{-2}) and active area 0.16 cm^2

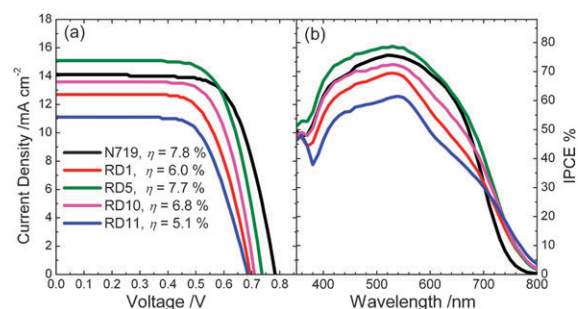| Dye	Dye loading/nmol cm^{-2}	J_{SC}/mA cm^{-2}	V_{OC}/V	FF	η (%)
RD1	295	12.744	0.694	0.68	6.0
RD5	216	15.084	0.737	0.69	7.7
RD10	253	13.612	0.710	0.70	6.8
RD11	291	11.159	0.685	0.67	5.1
N719	149	14.157	0.783	0.70	7.8

Fig. 2 (a) Current–voltage characteristics of **RD1**, **RD5**, **RD10**, **RD11** and **N719** measured under thick TiO_2 conditions (12 μm active layer + 3 μm scattering layer); (b) corresponding IPCE action spectra.
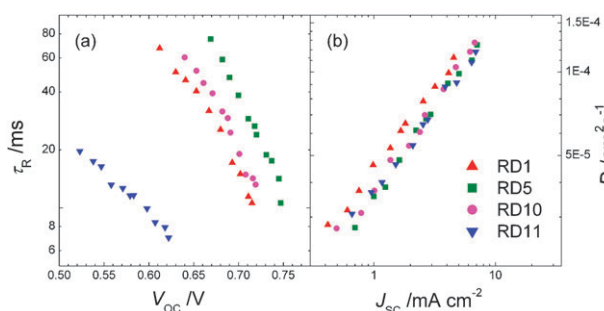

Fig. 3 Electron-transport properties: (a) recombination coefficient vs. V_{OC} and (b) diffusion coefficient vs. J_{SC} for DSSC devices made of **RD1**, **RD5**, **RD10** and **RD11**. The wavelengths are 632.8 nm for the bias light and 430 nm for the probe (ns pulse).

impedes the charge recombination, but the existence of the benzyl substituent in the imidazolyl ligand (**RD5**) might involve a hindrance to retard the charge recombination. In contrast, the system with a dimeric imidazolyl ligand (**RD11**) might increase the chance for charge recombination, so as to diminish the electron density in the conduction band of TiO_2. As a result, both V_{OC} and J_{SC} show the same order as we observed for τ_R.

Our results indicate that charge recombination plays a key role in cell performance. There are two charge recombinations: one is the reaction between the electrons in the conduction band of TiO_2 and I_3^- in the electrolyte (electron interception), and the other is the reaction between the conduction-band electrons and the dye cations (BET).[9] To investigate the kinetics of back transfer of electrons without involving an electrolyte, we measured the infrared TA kinetics[10] for each dye adsorbed on a thin-film sample. The dye molecules were excited with a fs pulse at 625 nm, and the conduction-band electrons were probed with another, delayed fs pulse at 4.9 μm. The resulting TA signals were obtained on varying the delay between the visible pump pulse and the IR probe pulse. Fig. 4 displays the normalized TA traces for **RD1**, **RD5**, **RD11** and **N719**. The transient of **N719** involves a rapid rise and then a slow rise approaching asymptotically an offset level within a ns range. The transients of the **RD**-series dyes exhibit, however, a rapid rise and a slow decay. The existence of a slow rise for the transient of **N719** indicates that there might exist an energy barrier between the excited state of the dye and the conduction band of TiO_2, and the excitation occurred near the band edge, whereas the absence of such a feature for the transients of all
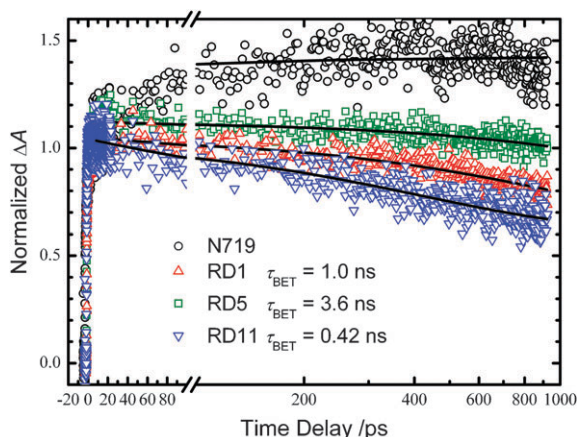
Fig. 4 Time-resolved profiles of infrared transient absorption of TiO_2 films (thickness 2 μm) sensitized with **RD1**, **RD5**, **RD11** and **N719**. The excitation and probe wavelengths are 625 nm and 4.9 μm, respectively.

other **RD** dyes indicates that the excitation energies were much above the energy barrier. The cyclic voltammetry measurements indicate that the LUMO level of **N719** is significantly below those of the **RD** dyes (Fig. S3†), consistent with our assumption.

The transient of **N719** does not decay in the observed ns region, whereas the transients of **RD1**, **RD5** and **RD11** exhibit a slow-decay feature with an offset for which the decay characteristics cannot be resolved on this time scale. The slow-decay components of the transients were fitted with time coefficients 1.0 ns for **RD1**, 3.6 ns for **RD5** and 0.42 ns for **RD11**. These results indicate that there exists a ns-BET process in the **RD** dyes that was non-observable in **N719**. The observed BET kinetics are consistent with HOMO levels showing a sequence of **RD11** > **RD1** > **RD5** > **N719** (Fig. S3†). Because the dye regeneration of a Ru system occurs typically on a μs scale,[11] the observed BET of the **RD** dyes on the ns scale are expected to play a role in cell performance. The BET kinetics were observed for thin-film samples that involved no electrolyte, but the trend of the BET decays is consistent with the variation of V_{OC} showing the order **N719** > **RD5** > **RD1** > **RD11** for the corresponding devices. Because **RD5** has a greater light-harvesting feature to enhance its J_{SC}, it compensates its V_{OC} loss to yield a cell performance comparable with that of **N719**.

In conclusion, we designed new heteroleptic ruthenium complexes containing benzimidazole substituents for application to dye-sensitized solar cells. These Ru complexes were synthesized according to a standard one-pot procedure with the corresponding heteroleptic ligands produced in only two simple steps. The corresponding devices show performances with the order **RD5** > **RD10** > **RD1** > **RD11**; the efficiency of power conversion of **RD5** is comparable with that of **N719**. The results obtained from photocurrent and photovoltage decays indicate that the electron lifetimes of the devices display a systematic trend **RD5** > **RD10** > **RD1** > **RD11**, which is consistent with the cell performance showing the same order. The observed charge-recombination kinetics reasonably explain

the order of V_{OC} to be **N719** > **RD5** > **RD10** > **RD1** > **RD11**. The IPCE action spectra of the devices account for the order of J_{SC} to be **RD5** > **N719** > **RD10** > **RD1** > **RD11**. Note that the molecular structure of **RD10** is similar to a highly efficient Ru sensitizer (**CBTR**) recently reported,[12] but the latter benzimidazyl ligand was coordinated with the N–C atoms involving more synthetic steps. We emphasize here that the ease of synthesis is an important factor to be considered in making a highly efficient sensitizer for future commercialization. Work is in progress along this line to design and to synthesize more efficient heteroleptic ruthenium complex sensitizers with superior light-harvesting ability and slower charge recombination.

Notes and references

1 (*a*) M. Grätzel, *Acc. Chem. Res.*, 2009, **42**, 1788; (*b*) H. J. Snaith, *Adv. Funct. Mater.*, 2010, **20**, 13.
2 (*a*) F. Gao, Y. Wang, D. Shi, J. Zhang, M. Wang, X. Jing, R. Humphry-Baker, P. Wang, S. M. Zakeeruddin and M. Grätzel, *J. Am. Chem. Soc.*, 2008, **130**, 10720; (*b*) C.-Y. Chen, J.-G. Chen, S.-J. Wu, J.-Y. Li, C.-G. Wu and K.-C. Ho, *Angew. Chem., Int. Ed.*, 2008, **47**, 7342; (*c*) J.-J. Kim, H. Choi, C. Kim, M.-S. Kang, H. S. Kang and J. Ko, *Chem. Mater.*, 2009, **21**, 5719.
3 (*a*) C.-W. Lee, H.-P. Lu, C.-M. Lan, Y.-L. Huang, Y.-R. Liang, W.-N. Yen, Y.-C. Liu, Y.-S. Lin, E. W.-G. Diau and C.-Y. Yeh, *Chem.–Eur. J.*, 2009, **15**, 1403; (*b*) H.-P. Lu, C.-L. Mai, C.-Y. Tsia, S.-J. Hsu, C.-P. Hsieh, C.-L. Chiu, C.-Y. Yeh and E. W.-G. Diau, *Phys. Chem. Chem. Phys.*, 2009, **11**, 10270; (*c*) H.-P. Lu, C.-Y. Tsai, W.-N. Yen, C.-P. Hsieh, C.-W. Lee, C.-Y. Yeh and E. W.-G. Diau, *J. Phys. Chem. C*, 2009, **113**, 20990.
4 (*a*) S. Ito, H. Miura, S. Uchida, M. Takata, K. Sumioka, P. Liska, P. Comte, P. Pechy and M. Grätzel, *Chem. Commun.*, 2008, 5194; (*b*) G. Zhang, H. Bala, Y. Cheng, D. Shi, X. Lv, Q. Yu and P. Wang, *Chem. Commun.*, 2009, 2198; (*c*) Z. Ning and H. Tian, *Chem. Commun.*, 2009, 5483.
5 (*a*) M. K. Nazeeruddin, F. De Angelis, S. Fantacci, A. Selloni, G. Viscardi, P. Liska, S. Ito, B. Takeru and M. Grätzel, *J. Am. Chem. Soc.*, 2005, **127**, 16835; (*b*) Q. Wang, S. Ito, M. Grätzel, F. Fabregat-Santiago, I. Mora-Seró, J. Bisquert, T. Bessho and H. Imai, *J. Phys. Chem. B*, 2006, **110**, 25210.
6 (*a*) C.-Y. Chen, M. Wang, J.-Y. Li, N. Pootrakulchote, L. Alibabaei, C. Ngoc-le, J.-D. Decoppet, J.-H. Tsai, C. Grätzel, C.-G. Wu, S. M. Zakeeruddin and M. Grätzel, *ACS Nano*, 2009, **3**, 3103; (*b*) Y. Cao, Y. Bai, Q. Yu, Y. Cheng, S. Liu, D. Shi, F. Gao and P. Wang, *J. Phys. Chem. C*, 2009, **113**, 6290.
7 Y. Li, M. K. Fung, Z. Xie, S.-T. Lee, L.-S. Hung and J. Shi, *Adv. Mater.*, 2002, **14**, 1317.
8 (*a*) L. Luo, C.-J. Lin, C.-Y. Tsai, H.-P. Wu, L.-L. Li, C.-F. Lo, C.-Y. Lin and E. W.-G. Diau, *Phys. Chem. Chem. Phys.*, 2010, **12**, 1064; (*b*) L. Luo, C.-J. Lin, C. S. Hung, C.-F. Lo, C.-Y. Lin and E. W.-G. Diau, *Phys. Chem. Chem. Phys.*, 2010, **12**, 12973.
9 C.-W. Chang, C. K. Chou, I.-J. Chang, Y.-P. Lee and E. W.-G. Diau, *J. Phys. Chem. C*, 2007, **111**, 13288.
10 C.-W. Chang, L. Luo, C.-K. Chou, C.-F. Lo, C.-Y. Lin, C.-S. Hung, Y.-P. Lee and E. W.-G. Diau, *J. Phys. Chem. C*, 2009, **113**, 11524.
11 A. B. F. Martinson, T. W. Hamann, M. J. Pellin and J. T. Hupp, *Chem.–Eur. J.*, 2008, **14**, 4458.
12 W.-C. Chang, H.-S. Chen, T.-Y. Li, N.-M. Hsu, Y. S. Tingare, C.-Y. Li, Y.-C. Liu, C. Su and W.-R. Li, *Angew. Chem., Int. Ed.*, 2010, DOI: 10.1002/anie.201001628, in press.